

# Boundary conditions in quantum mechanics on the discretized half-line

Gabor Kunstatter<sup>†</sup> and Jorma Louko<sup>‡</sup>

<sup>†</sup> *Department of Physics and Winnipeg Institute of Theoretical Physics,  
The University of Winnipeg,  
515 Portage Avenue, Winnipeg, Manitoba, Canada R3B 2E9  
[e-mail: g.kunstatter@uwinnipeg.ca]*

<sup>‡</sup> *School of Mathematical Sciences, University of Nottingham,  
Nottingham NG7 2RD, United Kingdom  
[e-mail: jorma.louko@nottingham.ac.uk]*

## Abstract

We investigate nonrelativistic quantum mechanics on the discretized half-line, constructing a one-parameter family of Hamiltonians that are analogous to the Robin family of boundary conditions in continuum half-line quantum mechanics. For classically singular Hamiltonians, the construction provides a singularity avoidance mechanism that has qualitative similarities with singularity avoidance encountered in loop quantum gravity. Applications include the free particle, the attractive Coulomb potential, the scale invariant potential and a black hole described in terms of the Einstein-Rosen wormhole throat. The spectrum is analyzed by analytic and numerical techniques. In the continuum limit, the full Robin family of boundary conditions can be recovered via a suitable fine-tuning but the Dirichlet-type boundary condition emerges as generic.

# 1 Introduction

It is often useful and sometimes necessary to study quantum mechanics on the half-line  $[0, \infty)$ . The boundary, which has been taken to be at the origin without loss of generality, can represent the location of a singularity in the potential or an infinite potential barrier (impenetrable wall) in the presence of an otherwise non-singular potential. The form of the Hamiltonian determines what conditions on the wave functions at the boundary lead to a quantization with unitary time evolution, if indeed such quantizations exist. Textbook accounts can be found in [1, 2] and accessible reviews in [3].

If the Hamiltonian is essentially self-adjoint, no boundary conditions are required. It may however happen that the Hamiltonian has a family of self-adjoint extensions, each specified by a boundary condition. As an example, consider a particle in a smooth potential. If the potential is sufficiently well-behaved at  $x \rightarrow \infty$  so that no boundary conditions are needed there, the self-adjoint extensions are parametrized by a parameter  $L \in \mathbb{R} \cup \{\infty\} \simeq S^1 \simeq \text{U}(1)$ , such that the corresponding boundary condition on the wave function is the Robin boundary condition,

$$\psi(0) + L\psi'(0) = 0 . \quad (1.1)$$

The special case  $L = 0$  gives the Dirichlet boundary condition,  $\psi(0) = 0$ , and the special case  $L = \infty$  gives the Neumann boundary condition,  $\psi'(0) = 0$ . All values of  $L$  make the time evolution unitary, and  $L$  may be physically interpreted in terms of the phase shift of a wave packet on its reflection at the origin.

From a purely mathematical point of view all the self-adjoint extensions are created equal, none are preferred. In most physical situations, however, Dirichlet boundary conditions seem to be considered ‘natural’. One argument to this end comes from regarding a singular potential or an infinite wall as a mathematical idealization of a physical situation in which the potential is regular [4]. Assuming that the Hamiltonian for the regular potential is already essentially self-adjoint and requires no boundary conditions, the ‘physical’ boundary conditions in the singular potential approximation may then be defined as those obtained when the regular potential approaches the singular one. It is a somewhat surprising mathematical fact that recovering in this limit anything other than the Dirichlet boundary conditions tends to require severe fine-tuning in the way in which the limit is taken [4].

The context of the foregoing discussion was conventional Schrödinger quantization. In this paper we investigate a similar issue of boundary conditions in polymer quantization, in which the continuous variable  $x \in \mathbb{R}_+ \cup \{0\}$  is replaced by a discrete variable and the inner product becomes a discrete sum rather than an integral [5, 6]. This quantization scheme arises most naturally in loop quantum gravity [7, 8]. The term “polymer” stems from that fact that the quantum states of the so-called “polymer particle representation” are mathematically ana-

loguous to the polymer-like excitations of quantum geometry [5]. Although we retain the loop quantum gravity motivated name, we stress that polymer quantization is a viable quantization procedure in its own right, unitarily inequivalent to Schrödinger quantization. It has been applied to a variety of systems, including the harmonic oscillator [5], the Coulomb potential [9], the scale invariant potential [10], and the Schwarzschild spacetime as described in terms of the dynamics of the Einstein-Rosen wormhole throat [11, 12]. In the last three of these systems the configuration space is the half-line, rather than the full real line, and the analyses in [9, 10, 11, 12] treat the restriction to a half-line by first polymer quantizing on the full real line and then considering separately the even and odd sectors, mimicking respectively the Neumann and Dirichlet boundary conditions in continuum. In the case of the even sector, a potential that is singular at the origin needs in addition to be regulated, and this was done by the Thiemann trick [13]. Most recently, Dirichlet boundary conditions were applied in the analysis of the statistical thermodynamics of a polymer particle in a box [14].

In this paper we construct a family of polymer Hamiltonians that is analogous to the Robin family of boundary conditions in Schrödinger quantization, and we analyze the continuum limit of these polymer theories. The construction does not rely on extending the polymer dynamics from half-line to full line, and it applies to potentials that are singular at the origin without a need to introduce a separate regularization for the potential. We shall show that the continuum limit of our family of polymer Hamiltonians does reproduce the Robin family of boundary conditions for the Schrödinger Hamiltonian. We shall further find that a fine-tuning of the polymer Hamiltonian in this limit is required in order to recover Schrödinger boundary conditions other than Dirichlet. The continuum Dirichlet boundary conditions hence emerge as generic when approached from polymer quantization, just as they emerge as generic when approached via regular potentials within Schrödinger quantization.

As concrete examples, we consider the following one-dimensional systems, each of which is motivated by specific physical applications:

1. The free particle in the presence of an infinitely high potential wall. This is the prototype for any discussion of quantum mechanics on the half line.
2. The attractive Coulomb potential. This describes the spherically symmetric sector of the hydrogen atom.
3. The scale invariant potential. This has applications in physics of polymers [15] and in molecular physics [16], and it also arises in the context of quantizing spherically symmetric black holes [17].
4. The Hamiltonian that describes the dynamics of the Einstein-Rosen wormhole throat [11, 12].

The paper is organized as follows: In Section 2 we present the general construction of our half-line polymer Hamiltonians for systems whose classical Hamiltonian is of the conventional nonrelativistic form,  $H = p^2 + V(x)$ . Sections 3, 4 and 5 apply this construction respectively to the free particle, the attractive Coulomb potential and the scale invariant potential. Section 6 addresses the Einstein-Rosen wormhole throat dynamics: in this system the classical kinetic term has a more complicated form, but we show that the construction of Section 2 has nevertheless a natural generalization. Section 7 presents a summary and brief concluding remarks.

We use throughout dimensionless units: for the Coulomb potential the configuration space coordinate is twice the Rydberg radial coordinate as in [9], and in the Einstein-Rosen throat theory the units are the Planck units as in [11, 12]. Complex conjugation is denoted by overline.

## 2 Polymer half-line quantization for nonrelativistic Hamiltonians

In this section we present our family of half-line polymer Hamiltonians for systems whose classical Hamiltonian consists of kinetic and potential terms of non-relativistic standard form. Subsection 2.1 recalls the key features of polymer quantization of this system on the full real line [5]. The half-line version is given in subsection 2.2.

### 2.1 Polymer real line

We consider a system whose classical phase space is  $\mathbb{R}^2 = \{(x, p)\}$  with the Poisson bracket  $\{x, p\} = 1$  and the Hamiltonian

$$H = p^2 + V(x) . \quad (2.1)$$

We assume the potential  $V$  to be defined for all  $x$  and real-valued.

The polymer Hilbert space is spanned by the basis states

$$\psi_{x_0}(x) = \begin{cases} 1, & x = x_0 \\ 0, & x \neq x_0 \end{cases} \quad (2.2)$$

with the inner product

$$(\psi_x, \psi_{x'}) = \delta_{x, x'}, \quad (2.3)$$

where the object on the right hand side is the Kronecker delta. The position operator  $\hat{x}$  acts by pointwise multiplication as

$$(\hat{x}\psi)(x) := x\psi(x), \quad (2.4)$$

and the family of translation operators  $\{\widehat{U}_\mu \mid \mu \in \mathbb{R}\}$  is defined as in Schrödinger quantization by

$$(\widehat{U}_\mu \psi)(x) := \psi(x + \mu). \quad (2.5)$$

In Schrödinger quantization the action of  $\widehat{U}_\mu$  (2.5) is weakly continuous in  $\mu$ , and the usual momentum operator  $\hat{p} := -i\partial_x$  can be defined in terms of the translation operator by  $\widehat{U}_\mu = e^{i\mu\hat{p}}$ . In polymer quantization the action of  $\widehat{U}_\mu$  is not weakly continuous in  $\mu$  and a similar definition of a momentum operator is not available. Instead, we now take  $\mu$  to be a fixed positive constant, understood as a fundamental length scale in the polymer quantum theory, and define the momentum operator and its square by

$$\hat{p} := \frac{1}{2i\mu}(\widehat{U}_\mu - \widehat{U}_\mu^\dagger), \quad (2.6a)$$

$$\hat{p}^2 := \frac{1}{\bar{\mu}^2}(2 - \widehat{U}_{\bar{\mu}} - \widehat{U}_{\bar{\mu}}^\dagger), \quad (2.6b)$$

where  $\bar{\mu} := 2\mu$ . The polymer Hamiltonian is defined to be

$$\widehat{H} := \widehat{T} + \widehat{V}, \quad (2.7)$$

where  $\widehat{V}$  acts by pointwise multiplication,

$$(\widehat{V}\psi)(x) := V(x)\psi(x), \quad (2.8)$$

and

$$\widehat{T} := \hat{p}^2 = \frac{1}{\bar{\mu}^2}(2 - \widehat{U}_{\bar{\mu}} - \widehat{U}_{\bar{\mu}}^\dagger). \quad (2.9)$$

$\widehat{H}$  is clearly symmetric. Its action decomposes the polymer Hilbert space into a continuum of separable superselection sectors, where each sector consists of wave functions supported on the regular  $\bar{\mu}$ -spaced lattice  $\{\Delta + m\bar{\mu} \mid m \in \mathbb{Z}\}$  and the parameter  $\Delta \in [0, \bar{\mu})$  parametrizes the sectors. A study of the deficiency indices [1] shows that  $\widehat{H}$  has at least one self-adjoint extension in each superselection sector. In particular, the Kato-Rellich theorem [1] can be applied as in [10] to show that  $\widehat{H}$  is essentially self-adjoint in every superselection sector in which the function  $V$  is bounded.

It is useful to write the Hilbert space of each superselection sector in terms of sequences. For concreteness, consider the superselection sector  $\Delta = 0$ . An orthonormal basis is given by  $\{\psi_{m\bar{\mu}} \mid m \in \mathbb{Z}\}$ . Writing  $\psi = \sum_m c_m \psi_{m\bar{\mu}}$ , the inner product reads  $(\psi^{(1)}, \psi^{(2)}) = \sum_m \overline{c_m^{(1)}} c_m^{(2)}$ , and the action of  $\widehat{H}$  reads

$$\widehat{H} \left( \sum_m c_m \psi_{m\bar{\mu}} \right) = \sum_m \left( \frac{2c_m - c_{m+1} - c_{m-1}}{\bar{\mu}^2} + V(m\bar{\mu})c_m \right) \psi_{m\bar{\mu}}. \quad (2.10)$$

The Hilbert space hence consists of the two-sided square summable sequences  $c := (c_m)_{m=-\infty}^{\infty}$ , and the action of  $\hat{H}$  reads

$$(\hat{H}c)_m = \frac{2c_m - c_{m+1} - c_{m-1}}{\bar{\mu}^2} + V(m\bar{\mu})c_m . \quad (2.11)$$

## 2.2 Polymer half-line

We wish to modify the polymer Hamiltonian (2.11) into a Hamiltonian in the Hilbert space of *one-sided* square-summable sequences.

We take the one-sided sequences to be of the form  $c := (c_m)_{m=1}^{\infty}$  and the inner product to read  $(d, c) = \sum_{m=1}^{\infty} \overline{d_m} c_m$ . We define the one-parameter family of modified Hamiltonians  $\{\hat{H}_\alpha \mid \alpha \in \mathbb{R}\}$  by

$$(\hat{H}_\alpha c)_m := \begin{cases} \frac{2c_m - c_{m+1} - c_{m-1}}{\bar{\mu}^2} + V(m\bar{\mu})c_m & \text{for } m > 1; \\ \frac{(2 - \alpha)c_1 - c_2}{\bar{\mu}^2} + V(\bar{\mu})c_1 & \text{for } m = 1. \end{cases} \quad (2.12)$$

Each  $\hat{H}_\alpha$  is symmetric, and it can be verified as with the two-sided sequences that each  $\hat{H}_\alpha$  has at least one self-adjoint extension. If  $V = 0$ , it can be explicitly verified that there are no nonvanishing normalizable solutions to  $\hat{H}_\alpha c = \pm ic$ , and in this case  $\hat{H}_\alpha$  is hence essentially self-adjoint. It follows by the Kato-Rellich theorem [1] that  $\hat{H}_\alpha$  is essentially self-adjoint whenever the set  $\{V(m\bar{\mu}) \mid m = 1, 2, \dots\}$  is bounded.

The motivation for the definition of  $(\hat{H}_\alpha c)_m$  by (2.12) is that  $(\hat{H}_\alpha c)_m$  agrees with  $(\hat{H}c)_m$  (2.11) for  $m \geq 1$  if we envisage there to be a fictitious lattice point at  $m = 0$  such that  $c_0 = \alpha c_1$ . This means that  $\alpha \in \mathbb{R}$  can be regarded as a lattice counterpart of the continuum theory self-adjoint extension parameter  $L$ . The case  $\alpha = 0$  is analogous to continuum Dirichlet, with the continuum boundary at  $m = 0$ . The cases  $\alpha = \pm 1$  are respectively analogous to the continuum Neumann and continuum Dirichlet, with the continuum boundary half-way between  $m = 0$  and  $m = 1$ .

Two comments are in order. First, given the definition (2.12), the coefficient of  $\overline{d_1} c_1$  in the inner product  $(d, c) = \sum_{m=1}^{\infty} \overline{d_m} c_m$  cannot be changed without losing symmetricity of  $\hat{H}_\alpha$ . Second, although the definition of  $\hat{H}_\alpha$  is motivated by a fictitious lattice point at  $m = 0$ , the actual definition involves  $V$  only at lattice points  $x = m\bar{\mu}$  with  $m \geq 1$ .  $\hat{H}_\alpha$  is hence well defined even if the classical potential is singular at  $x = 0$ .

## 3 Free particle

As the first example we consider the free particle,  $V = 0$ . We begin by recalling relevant facts from Schrödinger quantization on the half-line [1, 2, 3] and from

polymer quantization on the full real line [5]. We then analyze  $\widehat{H}_\alpha$  (2.12) and its continuum limit.

### 3.1 Schrödinger half-line

In Schrödinger quantization, the Hamiltonian operator of a free particle on the half-line is  $\widehat{H}_{\text{free}} := -d^2/dx^2$ , acting in the Hilbert space  $L_2(\mathbb{R}_+, dx)$ .  $\widehat{H}_{\text{free}}$  is symmetric and has a  $U(1) \simeq S^1$  of self-adjoint extensions, specified by the boundary condition (1.1).

The spectrum of each extension contains the positive continuum. The extensions with  $0 < L < \infty$  have in addition a discrete ground state of energy  $-L^{-2}$ . The spectral decomposition of the identity in terms of the eigenfunctions can be found in [18].

### 3.2 Polymer real line

Polymer quantization on the full real line can be analyzed by interpreting the two-sided square summable sequence  $c := (c_m)_{m=-\infty}^\infty$  as the coefficients in the Fourier expansion  $\chi(\varphi) = (2\pi)^{-1/2} \sum_m c_m e^{im\varphi}$  of the function  $\chi \in L_2(S^1)$ , so that in this realization  $(\widehat{H}\chi)(\varphi) = 2\bar{\mu}^{-2} (1 - \cos \varphi) \chi(\varphi)$ . It is immediate that  $\widehat{H}$  is essentially self-adjoint and its spectrum is the continuum  $(0, 4\bar{\mu}^{-2})$ .

### 3.3 Polymer half-line

The half-line polymer Hamiltonian is given by  $\widehat{H}_\alpha$  (2.12) with  $V = 0$ . As noted above,  $\widehat{H}_\alpha$  is essentially self-adjoint.

#### 3.3.1 Spectrum

We wish to find the spectrum.

Let  $E \in \mathbb{R}$  denote the energy eigenvalue, which may be a proper eigenvalue in the discrete spectrum or an improper eigenvalue in the continuous spectrum. The eigenvalue equation reads

$$\widehat{H}_\alpha c = Ec . \quad (3.1)$$

If  $E \neq 0$  and  $E \neq 4\bar{\mu}^{-2}$ , the solution to (3.1) as a difference equation is

$$c_m = aA_+^m + bA_-^m , \quad (3.2)$$

where  $a$  and  $b$  are constants,

$$A_\pm := \left(1 - \frac{1}{2}\bar{\mu}^2 E\right) \pm \sqrt{\left(1 - \frac{1}{2}\bar{\mu}^2 E\right)^2 - 1} , \quad (3.3)$$

and evaluating (3.1) at the lattice point  $m = 1$  by (2.12) shows that (3.2) must in addition satisfy

$$c_2 = (2 - \alpha - \bar{\mu}^2 E) c_1 , \quad (3.4)$$

so that for each  $\alpha$  there is only one linearly independent solution. If  $E = 0$  or  $E = 4\bar{\mu}^{-2}$ , we proceed similarly, finding that the only linearly independent solution to (3.1) as a difference equation is

$$c_m = \begin{cases} \alpha + (1 - \alpha)m & \text{for } E = 0; \\ (-1)^m [\alpha - (1 + \alpha)m] & \text{for } E = 4\bar{\mu}^{-2}. \end{cases} \quad (3.5)$$

The spectrum is now found by considering the normalizability properties of these solutions.

Suppose first that  $0 < E < 4\bar{\mu}^{-2}$ . We parametrize  $E$  as

$$\bar{\mu}^2 E = 4 \sin^2(\theta/2) , \quad (3.6)$$

where  $0 < \theta < \pi$ . From (3.3) we then have  $A_{\pm} = e^{\pm i\theta}$ , and from (3.4) it follows that the solution reads

$$c_m = \sin(m\theta + \delta) , \quad (3.7)$$

where  $\delta$  is determined in terms of  $\alpha$  and  $\theta$  from

$$\cot \delta = \frac{1}{\alpha \sin \theta} - \cot \theta , \quad (3.8)$$

understood for  $\alpha = 0$  in the limiting sense  $\delta = 0$ . Note that  $\delta$  is unique up to an additive integer multiple of  $\pi$ . Note also that in the special cases  $\alpha = 0$ ,  $\alpha = 1$  and  $\alpha = -1$ , we have respectively  $\delta = 0$ ,  $\delta = (\pi - \theta)/2$  and  $\delta = -\theta/2$ . As the solutions are oscillatory at  $m \rightarrow \infty$ , they are lattice analogues of plane waves, belonging to the continuous spectrum.

Suppose then that  $E < 0$ . We now have  $A_+ > 1$  and  $0 < A_- < 1$ , and avoiding an exponential divergence at  $m \rightarrow \infty$  in (3.2) requires  $a = 0$ . Matching to (3.4) is possible iff  $\alpha > 1$ , and  $E$  is then uniquely determined in terms of  $\alpha$  by

$$E = (2 - \alpha - \alpha^{-1})\bar{\mu}^{-2} . \quad (3.9)$$

The solution is the normalizable, proper eigenstate  $c_m = \alpha^{-m}$ .

Suppose next that  $E > 4\bar{\mu}^{-2}$ . A similar analysis shows that a solution exists iff  $\alpha < -1$ ,  $E$  is uniquely determined in terms of  $\alpha$  by (3.9), and the solution is the normalizable, proper eigenstate  $c_m = \alpha^{-m}$ .

Suppose finally that  $E = 0$  or  $E = 4\bar{\mu}^{-2}$ . As the solutions (3.5) are not normalizable, these special values of  $E$  are not proper eigenvalues, and as points of measure zero they do not contribute to the spectrum.



We summarize. For any  $\alpha$ , the spectrum contains the band  $(0, 4\bar{\mu}^{-2})$  of improper, Dirac-delta-normalizable eigenstates, given by (3.7) with (3.6) and (3.8). For each  $\alpha$  such that  $|\alpha| > 1$ , there exists in addition a unique proper eigenstate, given by  $c_m = \alpha^{-m}$  and having the eigenvalue (3.9). For  $\alpha > 1$  the proper eigenstate is a ground state at  $E < 0$ , below the continuous band, and for  $\alpha < -1$  it is a highly excited state at  $E > 4\bar{\mu}^{-2}$ , above the continuous band.

We note that the special case  $\alpha = 1$  of our free particle Hamiltonian is obtained from the family of discrete Hamiltonians (2.12) in [19] with the choices  $B(x) = D(x) = 1$  for  $x > 0$  and  $B(0) = 1$ , where the discrete configuration variable  $x$  of [19] is such that  $x = 0$  corresponds to our  $m = 1$ . As discussed above, the spectrum with this value of  $\alpha$  consists of the continuum band  $(0, 4\bar{\mu}^{-2})$  and does not contain a bound state. This exemplifies the observation made at the end of subsection 2.2 that even though we invoked a fictitious  $m = 0$  lattice point to motivate the definition of the Hamiltonian, the actual definition does not refer to this lattice point and the value of the wave function at the fictitious lattice point never enters the theory: in the formulation of [19] the  $\alpha = 1$  theory is indeed constructed without a motivation via fictitious lattice points.

### 3.3.2 Continuum limit

We now show that the full one-parameter family of continuum Schrödinger quantizations can be recovered in the continuum limit.

The key for taking the limit is to make  $\alpha$  dependent on  $\bar{\mu}$  in a suitable way. We introduce a parameter  $L_P \in \mathbb{R} \cup \{\infty\}$ , which is considered independent of  $\bar{\mu}$ , and we choose

$$\alpha = \begin{cases} 0 & \text{for } L_P = 0; \\ 1 & \text{for } L_P = \infty; \\ \frac{1}{1 - (\bar{\mu}/L_P)} & \text{otherwise,} \end{cases} \quad (3.10)$$

which is well defined for sufficiently small  $\bar{\mu}$  when  $L_P$  is in the interval  $(0, \infty)$ , and for all  $\bar{\mu}$  when  $L_P$  takes other values. When interpreted in terms of the fictitious lattice point at  $m = 0$  for which  $c_0 = \alpha c_1$ , (3.10) amounts to

$$\begin{aligned} c_0 + L_P \frac{(c_1 - c_0)}{\bar{\mu}} &= 0 & \text{for } L_P \neq \infty; \\ \frac{(c_1 - c_0)}{\bar{\mu}} &= 0 & \text{for } L_P = \infty. \end{aligned} \quad (3.11)$$

Comparison of (1.1) and (3.11) suggests that the polymer theory should reduce to the continuum theory with  $L = L_P$  as  $\bar{\mu} \rightarrow 0$ . We shall verify that it does.

Let first  $0 < L_P < \infty$  and focus on the ground state. By (3.9), the ground state energy is given by  $E = -L_P^{-2} + O(\bar{\mu})$ , and the ground state wave function

can be written in terms of the discrete distance coordinate  $x = m\bar{\mu}$  as

$$\psi(x) := c_{x/\bar{\mu}} = \left(1 - \frac{\bar{\mu}}{L_P}\right)^{x/\bar{\mu}} = e^{-x/L_P} + O(\bar{\mu}), \quad (3.12)$$

where in the last expression  $L_P$  and  $x$  are considered independent of  $\bar{\mu}$ . In the limit  $\bar{\mu} \rightarrow 0$ , we therefore recover the ground state energy and the ground state wave function of the continuum theory with  $L = L_P$ .

Let then  $L_P$  be arbitrary and consider energies in the continuous band. For fixed  $E$ , (3.6) and (3.8) give

$$\delta = \begin{cases} 0 & \text{for } L_P = 0; \\ \frac{1}{2}\pi + O(\bar{\mu}) & \text{for } L_P = \infty; \\ -\arctan(L_P\sqrt{E}) + O(\bar{\mu}) & \text{otherwise,} \end{cases} \quad (3.13)$$

and

$$\psi(x) := c_{x/\bar{\mu}} = \sin((\theta/\bar{\mu})x + \delta) = \sin(\sqrt{E}x + \delta) + O(\bar{\mu}^3). \quad (3.14)$$

In the limit  $\bar{\mu} \rightarrow 0$ , we therefore recover the continuum theory wave functions with  $L = L_P$ .

We emphasize that the fine-tuning of  $\alpha$  as a function of  $\bar{\mu}$  in (3.10) is essential. If the limit  $\bar{\mu} \rightarrow 0$  is instead taken with fixed  $\alpha$ , the choice  $\alpha = 1$  (corresponding to  $L_P = \infty$  in (3.10)) gives the Neumann continuum theory,  $L = \infty$ , while any other choice for  $\alpha$  (corresponding to  $L_P \rightarrow 0$  in (3.10)) gives the Dirichlet continuum theory,  $L = 0$ .

## 4 Coulomb potential

As the next example, we consider the attractive Coulomb potential,  $V(x) = -1/x$ . A new feature is that this potential is singular at  $x = 0$ .

### 4.1 Schrödinger half-line

In Schrödinger quantization [20], the Hamiltonian has a one-parameter family of self-adjoint extensions, specified by a boundary condition at  $x = 0$ . The boundary condition does not take the Robin form (1.1) but reads instead

$$(\tilde{L} - \Psi(1) - \Psi(2)) \psi(0) + \lim_{x \rightarrow 0} \left( \frac{\psi(x) - \psi(0)}{x} + \psi(0) \ln x \right) = 0, \quad (4.1)$$

where  $\psi$  is the wave function,  $\Psi$  is the digamma function [21] and  $\tilde{L} \in \mathbb{R} \cup \{\infty\}$  is the parameter. The second term in (4.1) can be understood as a logarithm-corrected first derivative, where the correction must be included because of the singularity of the potential at  $x \rightarrow 0$ .

The spectrum consists of the positive continuum and a countable number of proper negative eigenvalues. Writing  $s := 1/\sqrt{-4E}$  for  $E < 0$ , the eigenvalues are given by the solutions to

$$\tilde{L} = \Psi(1 - s) - \ln s + \frac{1}{2s} . \quad (4.2)$$

The solutions to (4.2) with  $\tilde{L} = \infty$  are  $s = 1, 2, 3, \dots$ , coming from the simple poles of  $\Psi$  at non-positive integers. This extension is analogous to the Dirichlet boundary condition for regular potentials, and it arises via a limiting prescription from regularized potentials that make the three-dimensional attractive Coulomb Hamiltonian essentially self-adjoint [20]. This is the extension that yields the textbook spectrum, realized in nature.

We note in passing that if physical dimensions are restored,  $\tilde{L}$  has an interpretation as an inverse length scale. Using  $\tilde{L}$ , rather than the associated length scale  $1/\tilde{L}$  [20], is convenient for us because the spectrum changes smoothly across  $\tilde{L} = 0$ . The only discontinuous change in the spectrum in terms of  $\tilde{L}$  occurs when  $\tilde{L} \rightarrow \infty$  through positive values: in this limit the ground state descends to  $-\infty$  and disappears.

## 4.2 Polymer half-line

The half-line polymer Hamiltonian is given by  $\hat{H}_\alpha$  (2.12) with  $V(m\bar{\mu}) = -1/(m\bar{\mu})$ . As noted in subsection 2.2, the boundedness of  $V$  over the lattice points shows that  $\hat{H}_\alpha$  is essentially self-adjoint.

We focus on a numerical study of the proper eigenvalues in the limit  $\bar{\mu} \rightarrow 0$ . The numerical scheme is as described in [9] except that the boundary condition to shoot for is now  $c_0 = \alpha c_1$ .

The key is again to make  $\alpha$  depend on  $\bar{\mu}$  in a suitable way. Motivated by the continuum boundary condition (4.1), we introduce a parameter  $\tilde{L}_P \in \mathbb{R} \cup \{\infty\}$ , and we choose

$$\alpha = \begin{cases} 0 & \text{for } \tilde{L}_P = \infty; \\ \frac{1}{1 - \bar{\mu}(\tilde{L}_P - \Psi(1) - \Psi(2) + \ln \bar{\mu})} & \text{otherwise,} \end{cases} \quad (4.3)$$

which is well defined for sufficiently small  $\bar{\mu}$  with any fixed value of  $\tilde{L}_P$ . Numerical results for the lowest three eigenvalues in terms of  $\tilde{L}_P$  are shown in Table 1. Numerical accuracy allows us to probe values of  $\bar{\mu}$  down to  $10^{-5}$ .

For  $\tilde{L}_P = \infty$ , we find that the polymer eigenenergies converge to those of the Schrödinger theory with  $\tilde{L} = \infty$ . For other values of  $\tilde{L}_P$ , we find that the polymer eigenenergies converge to those of a Schrödinger theory with  $\tilde{L} - \tilde{L}_P \approx 0.423$ . While we do not have an analytic explanation for this shift in  $\tilde{L} - \tilde{L}_P$ , we note that within our numerical accuracy the shift coincides with the constant  $\Psi(2) \approx$

$s_0$

$\tilde{L}_P$ or $\tilde{L}$	10	4/5	0	-1	-10	$\infty$
$\tilde{\mu} = 1$	–	0.1091	0.5745	0.7983	0.9934	$1 + 2.9 \times 10^{-2}$
$\tilde{\mu} = 10^{-1}$	0.0290	0.4475	0.5483	0.6549	0.9168	$1 + 3.1 \times 10^{-4}$
$\tilde{\mu} = 10^{-2}$	0.0636	0.4317	0.5225	0.6250	0.9073	$1 + 3.1 \times 10^{-6}$
$\tilde{\mu} = 10^{-3}$	0.0660	0.4279	0.5178	0.6202	0.9062	$1 + 3.1 \times 10^{-8}$
$\tilde{\mu} = 10^{-4}$	0.066170755	0.4273310795	0.517072743	0.619510329	0.906040222	$1 + 3.1 \times 10^{-10}$
$\tilde{\mu} = 10^{-5}$	0.066190491	0.4272479722	0.516979832	0.619423583	0.906025030	$1 + 3.1 \times 10^{-12}$
Schrödinger	0.0631	0.3814	0.4696	0.5785	0.9022	1
$\tilde{L}_P - \tilde{L}_{\text{eff}}$						
$\tilde{\mu} = 10^{-3}$	0.397491563	0.4287638124	0.4303204240	0.431360980	0.44340833	–
$\tilde{\mu} = 10^{-4}$	0.419935473	0.4236415186	0.4237432260	0.423857416	0.42477493	–
$\tilde{\mu} = 10^{-5}$	0.422522628	0.4228930728	0.4229032450	0.422914658	0.42300644	–

$s_1$

$\tilde{L}_P$ or $\tilde{L}$	10	4/5	0	-1	-10	$\infty$
$\tilde{\mu} = 1$	1.06769	1.436	1.645	1.806	1.9804	$2 + 1.5 \times 10^{-2}$
$\tilde{\mu} = 10^{-1}$	1.09386	1.482	1.571	1.668	1.9172	$2 + 1.6 \times 10^{-4}$
$\tilde{\mu} = 10^{-2}$	1.09981	1.463	1.545	1.638	1.9079	$2 + 1.6 \times 10^{-6}$
$\tilde{\mu} = 10^{-3}$	1.10024	1.459	1.540	1.634	1.9068	$2 + 1.6 \times 10^{-8}$
$\tilde{\mu} = 10^{-4}$	1.100263034	1.45830016	1.539302314	1.632903508	1.90664102	$2 + 1.6 \times 10^{-10}$
$\tilde{\mu} = 10^{-5}$	1.100263299	1.45821961	1.539214395	1.632821310	1.90662595	$2 + 1.6 \times 10^{-12}$
Schrödinger	1.09630	1.417	1.496	1.595	1.9029	2
$\tilde{L}_P - \tilde{L}_{\text{eff}}$						
$\tilde{\mu} = 10^{-3}$	0.420413025	0.4306943397	0.4307488453	0.436817400	0.44358639	–
$\tilde{\mu} = 10^{-4}$	0.422779633	0.4237041296	0.4237847082	0.423885292	0.42478657	–
$\tilde{\mu} = 10^{-5}$	0.422806855	0.4228993154	0.4229073956	0.422917448	0.42300773	–

$s_2$

$\tilde{L}_P$ or $\tilde{L}$	10	4/5	0	-1	-10	$\infty$
$\tilde{\mu} = 1$	2.05400	2.4374	2.6463	2.8039	2.9755	$3 + 1.033 \times 10^{-2}$
$\tilde{\mu} = 10^{-1}$	2.09419	2.4851	2.5734	2.6690	2.9172	$3 + 1.042 \times 10^{-4}$
$\tilde{\mu} = 10^{-2}$	2.10026	2.4653	2.5467	2.6398	2.9080	$3 + 1.042 \times 10^{-6}$
$\tilde{\mu} = 10^{-3}$	2.10069	2.4613	2.5421	2.6351	2.9069	$3 + 1.042 \times 10^{-8}$
$\tilde{\mu} = 10^{-4}$	2.100712343	2.4607015522	2.54141508	2.63445759	2.90674777	$3 + 1.042 \times 10^{-10}$
$\tilde{\mu} = 10^{-5}$	2.100712544	2.4606208222	2.54132730	2.63437572	2.90673263	$3 + 1.042 \times 10^{-12}$
Schrödinger	2.09672	2.4193	2.4987	2.5970	2.9030	3
$\tilde{L}_P - \tilde{L}_{\text{eff}}$						
$\tilde{\mu} = 10^{-3}$	0.420509240	0.4296974160	0.4306588703	0.431510579	0.44284175	–
$\tilde{\mu} = 10^{-4}$	0.422787147	0.4237079042	0.4237880518	0.423888137	0.42479883	–
$\tilde{\mu} = 10^{-5}$	0.422807636	0.4228997124	0.4229077629	0.422917713	0.42300750	–

Table 1: The table shows numerical results for the lowest three eigenenergies in the Coulomb potential, in the polymer theory as a function of the parameter  $\tilde{L}_P$  and the scale  $\tilde{\mu}$ , and in the Schrödinger theory as a function of the parameter  $\tilde{L}$ . The shown quantities  $s_0$ ,  $s_1$  and  $s_2$  parametrize the eigenenergies  $E_0$ ,  $E_1$  and  $E_2$  by  $s = 1/\sqrt{-4E}$ . The last three rows for each  $s_i$  show the values of  $\tilde{L}_P - \tilde{L}_{\text{eff}}$  such that the Schrödinger eigenvalue with  $\tilde{L} = \tilde{L}_{\text{eff}}$  equals the corresponding polymer eigenenergy. Note the convergence of  $\tilde{L}_P - \tilde{L}_{\text{eff}}$  to 0.423 with decreasing  $\tilde{\mu}$ , within the numerical accuracy.

0.4227843351 that appears in (4.1) and (4.3). Examining whether this coincidence continues to hold beyond three decimal places would require numerical work beyond  $\bar{\mu} = 10^{-5}$ .

If the limit  $\bar{\mu} \rightarrow 0$  is taken with any fixed value of  $\alpha$ , the relation (4.3) shows that the numerical results in Table 1 are consistent with convergence to the continuum theory with  $\tilde{L} = \infty$ .

## 5 Scale invariant potential

We next consider the scale invariant potential,  $V(x) = -\lambda/x^2$ , where  $\lambda$  is a real-valued constant. Although we work in dimensionless variables, we note that  $\lambda$  remains dimensionless even when physical dimensions are restored, and  $\lambda$  is hence a pure number whose value is significant regardless any unit choices. That the coupling constant is dimensionless is the special property of a scale invariant potential.

### 5.1 Schrödinger half-line

Schrödinger quantization of the system is reviewed in [10]. For  $\lambda \leq -3/4$  the Hamiltonian is essentially self-adjoint and the spectrum consists of the positive continuum. For  $\lambda > -3/4$  the self-adjoint extensions are specified by a parameter that takes values in  $U(1) \simeq S^1$ , and the spectrum of each extension contains the positive continuum but discrete negative eigenenergies can also exist. We shall recall here relevant facts about the cases in which discrete eigenenergies do exist.

For  $\lambda > 1/4$ , each extension has a countable tower of proper eigenenergies, given by

$$E_n = -\exp\left[2(\gamma - \pi n)/\sqrt{\lambda - (1/4)}\right], \quad n \in \mathbb{Z}, \quad (5.1)$$

where  $\gamma \in [0, \pi)$  is the parameter specifying the extension. The discrete spectrum is unbounded below,  $E_n \rightarrow -\infty$  as  $n \rightarrow -\infty$ , and it accumulates to 0 from below,  $E_n \rightarrow 0_-$  as  $n \rightarrow \infty$ .

For  $\lambda = 1/4$ , one of the extensions has no discrete eigenenergies but the rest have exactly one negative eigenenergy each.

For  $-3/4 < \lambda < 1/4$ , there is an open interval of extensions that have exactly one negative eigenenergy each. The remaining extensions have no discrete eigenenergies.

### 5.2 Polymer half-line

The half-line polymer Hamiltonian is given by  $\hat{H}_\alpha$  (2.12) with  $V(m\bar{\mu}) = -\lambda/(m\bar{\mu})^2$ . The boundedness of  $V$  over the lattice points again implies that  $\hat{H}_\alpha$  is essentially self-adjoint.

We again focus on a numerical study of the discrete eigenvalues. Because of the scale invariance of the potential, the polymer eigenvalues depend on  $\bar{\mu}$  only through the overall factor  $\bar{\mu}^{-2}$ . The question to be examined hence is how the combination  $\bar{\mu}^2 E$  depends on  $\lambda$ .

Because of the strong singularity of the continuum potential at  $x \rightarrow 0$ , it is not clear how the Schrödinger theory self-adjointness boundary conditions [10] might motivate a value of  $\alpha$  in our polymer Hamiltonian. We hence take  $\alpha = \tan \chi$ , where  $\chi \in [0, \pi)$ , allowing  $\chi = \pi/2$  to be considered as a limiting case. The numerical implementation is as in [10] except that the boundary condition to shoot for is

$$c_0 \cos \chi - c_1 \sin \chi = 0. \quad (5.2)$$

For  $\lambda \gtrsim 2$ , we find a tower of negative eigenenergies  $E_0 < E_1 < E_2 < \dots < 0$ . We have followed the tower up to  $E_6$  but slowness of the numerics has not enabled us to examine whether the tower terminates. Starting at  $\chi = 0$  and increasing  $\chi$ ,  $E_0$  first migrates downwards and then disappears at  $\chi \approx \pi/2$ ; slowness of the numerics has not enabled us to examine whether this disappearance happens by descent to  $-\infty$  or by some other mechanism. The excited states  $E_n$ ,  $n > 0$ , migrate down smoothly, meeting at  $\chi \rightarrow \pi$  with  $E_{n-1}$  at  $\chi = 0$ . Graphs for  $E_3$  in terms of  $\chi$  are shown in Figure 1 for  $\lambda = 4$  and  $\lambda = 8$ .

When  $\lambda$  decreases towards 0, the numerics becomes slow. Outside the interval  $\pi/4 < \chi < \pi/2$  we have found no evidence that any eigenstates would survive. Within the interval  $\pi/4 < \chi < \pi/2$ , however, comparison with the free particle polymer theory of Section 3 suggests that the ground state should persist as  $\lambda \rightarrow 0$  and tend to that of the corresponding  $\lambda = 0$  theory, given by

$$E_0 = \frac{2}{\bar{\mu}^2} \left( -1 + \frac{1}{\sin 2\chi} \right), \quad (5.3)$$

and we find numerical evidence that this indeed happens. A sample plot is shown in Figure 2.

If the lowest few states are excluded, the eigenenergies for  $\lambda \gtrsim 2$  are a good fit to the continuum eigenenergy formula (5.1), as shown in Figure 3. The continuum parameter  $\gamma$  is an increasing function of  $\chi$ , and for large  $\lambda$  it is slowly varying except when  $\chi$  is close to  $\pi/2$ .

## 6 Einstein-Rosen wormhole throat

As the final example, we study the interior dynamics of the eternal Schwarzschild black hole, adopting as the configuration variable the area of the Einstein-Rosen wormhole throat and as the time parameter the proper time of a comoving observer at the throat [22, 23, 24].

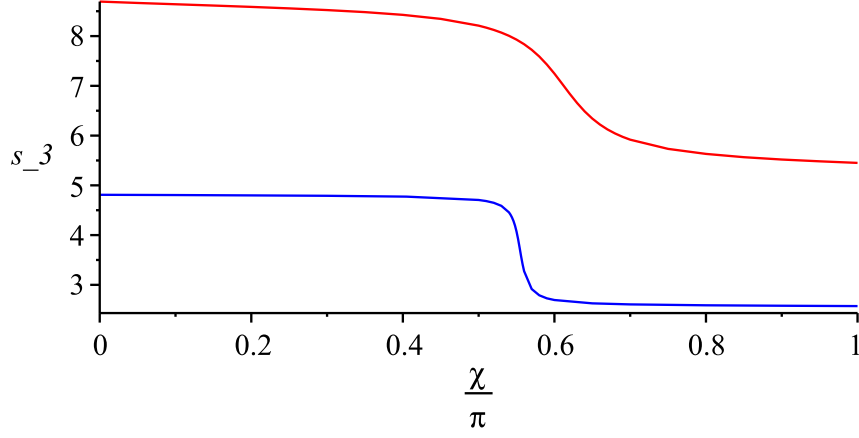


Figure 1: Scale invariant potential.  $s_3 := -\ln(-\bar{\mu}^2 E_3)$  is shown as a function of  $\chi$  for  $\lambda = 4$  (upper curve, red) and for  $\lambda = 8$  (lower curve, blue).

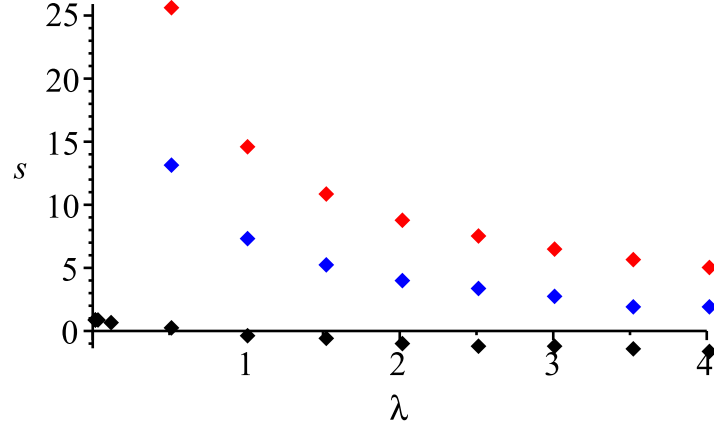


Figure 2: Scale invariant potential. Values of  $s_n := -\ln(-\bar{\mu}^2 E_n)$  are shown as a function of  $\lambda$  for  $\chi = \pi/3$ , for  $n = 0$  (low, black),  $n = 1$  (middle, blue) and  $n = 2$  (top, red). As  $\lambda \rightarrow 0$ ,  $s_0$  approaches the value of the  $\lambda = 0$  polymer theory,  $-\ln(-2 + 4/\sqrt{3}) \approx 1.11731$ , and the excited states disappear.

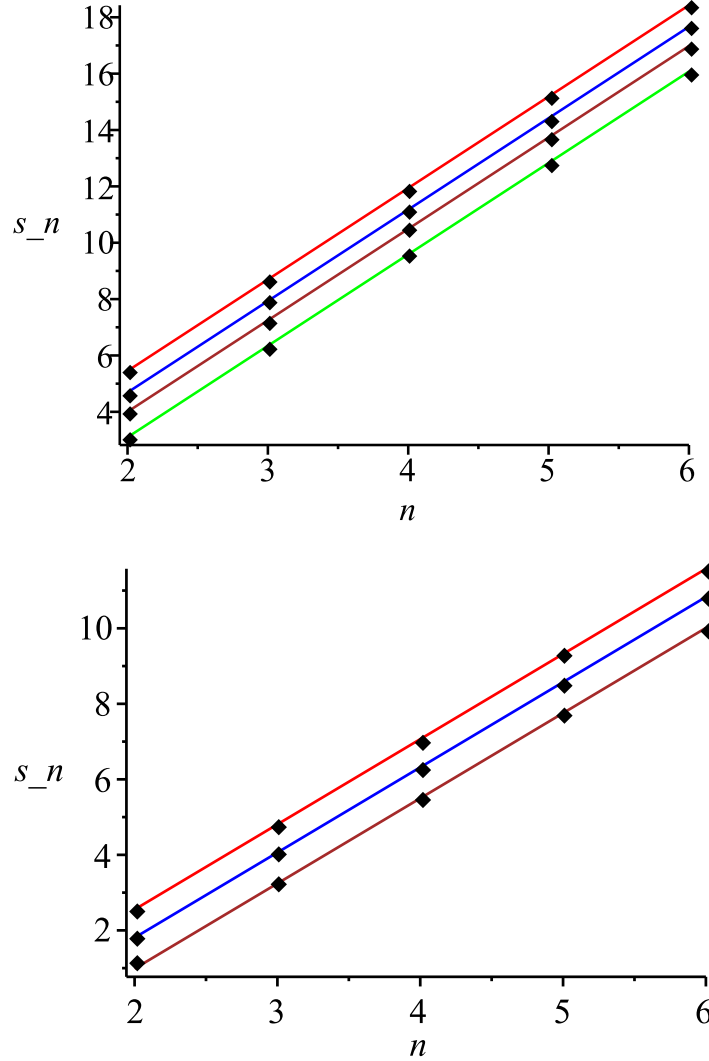


Figure 3: Scale invariant potential. Values of  $s_n := -\ln(-\bar{\mu}^2 E_n)$ ,  $2 \leq n \leq 6$ , are shown for different values of  $\chi$ , with a linear regression fit to the continuum formula (5.1). Upper diagram shows  $\lambda = 4$  and the lines from top to bottom are with  $\chi = 0$  (red),  $\chi = 0.55\pi$  (blue),  $\chi = 0.60\pi$  (brown) and  $\chi = 0.65\pi$  (green). Lower diagram shows  $\lambda = 8$  and the lines from top to bottom are with  $\chi = 0$  (red),  $\chi = 0.55\pi$  (blue) and  $\chi = 0.56\pi$  (brown).



## 6.1 Schrödinger half-line

Following [11], we take the classical phase space to be  $(\phi, \Pi)$ , where the positive-valued configuration coordinate  $\phi$  is the square of the wormhole throat area-radius and  $\Pi$  is the real-valued conjugate momentum. The classical Hamiltonian is given by

$$H = \frac{1}{2} \phi^{1/2} (4\Pi^2 + 1) . \quad (6.1)$$

We take the wave functions in Schrödinger quantization to be square integrable functions of  $\phi$  in the measure  $d\phi$ . For reasons that will emerge in the polymer theory, we consider the quantum Hamiltonian with the symmetric ordering

$$\hat{H}_{\text{Schr}} = \frac{1}{2} \left( -4 \frac{\partial}{\partial \phi} \phi^{1/2} \frac{\partial}{\partial \phi} + \phi^{1/2} \right) . \quad (6.2)$$

It is shown in [11, 24] that the self-adjoint extensions of  $\hat{H}_{\text{Schr}}$  are labelled by the parameter  $\theta \in [0, \pi)$  such that

$$\psi(\phi) = [1 + O(\phi^{3/2})] \sin \theta + \phi^{1/2} [1 + O(\phi^{3/2})] \cos \theta , \quad (6.3)$$

or equivalently

$$\psi(0) \cos \theta - \left( \lim_{\phi \rightarrow 0} \frac{\psi(\phi) - \psi(0)}{\phi^{1/2}} \right) \sin \theta = 0 , \quad (6.4)$$

so that  $\theta = 0$  is analogous to Dirichlet and  $\theta = \pi/2$  is analogous to Neumann. The spectrum of each self-adjoint extension is discrete and bounded below. Further analytic and numerical results on the spectrum are given in [11, 24].

## 6.2 Polymer real line

As the kinetic term of the classical Hamiltonian (6.1) does not have the conventional form of (2.1), the polymer quantization prescription of Section 2 must be suitably generalized. We now recall the results of [11] for the situation where  $\phi$  is polymer quantized on the full real line.

We polymerize the pair  $(\phi, \Pi)$  as the pair  $(x, p)$  in subsection 2.1, letting  $\phi$  take all real values, defining the basis states

$$\psi_{\phi_0}(\phi) = \begin{cases} 1, & \phi = \phi_0 \\ 0, & \phi \neq \phi_0 \end{cases} \quad (6.5)$$

with the inner product

$$(\psi_\phi, \psi_{\phi'}) = \delta_{\phi, \phi'} , \quad (6.6)$$

and the operators

$$(\hat{\phi}\psi)(\phi) := \phi\psi(\phi), \quad (6.7a)$$

$$(\hat{U}_\mu\psi)(\phi) := \psi(\phi + \mu), \quad (6.7b)$$

$$\hat{\Pi} := \frac{1}{2i\mu}(\hat{U}_\mu - \hat{U}_\mu^\dagger), \quad (6.7c)$$

where the positive constant  $\mu$  is again the fundamental polymer length scale. The polymer counterpart of the Schrödinger Hamiltonian (6.8) is taken to be

$$\hat{H} = \frac{1}{2} \left( 4\hat{\Pi}\hat{\phi}^{1/2}\hat{\Pi} + \hat{\phi}^{1/2} \right). \quad (6.8)$$

where the operator  $\hat{\phi}^{1/2}$  is defined by

$$(\hat{\phi}^{1/2}\psi)(\phi) := |\phi|^{1/2} \psi(\phi). \quad (6.9)$$

Specialising to the superselection sector in which  $\phi$  is confined to the lattice  $\{m\bar{\mu} \mid m \in \mathbb{Z}\}$  with  $\bar{\mu} := 2\mu$ , and writing  $\psi = \sum_m c_m \psi_{m\bar{\mu}}$ , the action of  $\hat{H}$  on the two-sided square-summable sequence  $c := (c_m)_{m=-\infty}^\infty$  reads

$$\begin{aligned} (\hat{H}c)_m = \frac{2}{\bar{\mu}^{3/2}} & \left[ \left( \left| m + \frac{1}{2} \right|^{1/2} + \left| m - \frac{1}{2} \right|^{1/2} + \frac{1}{4}\bar{\mu}^2 |m|^{1/2} \right) c_m \right. \\ & \left. - \left| m + \frac{1}{2} \right|^{1/2} c_{m+1} - \left| m - \frac{1}{2} \right|^{1/2} c_{m-1} \right]. \end{aligned} \quad (6.10)$$

It follows that the polymer Hilbert space breaks further into the even superselection sector, in which  $c_m = c_{-m}$ , and the odd superselection sector, in which  $c_m = -c_{-m}$ . In the limit  $\bar{\mu} \rightarrow 0$ , it is found numerically [11] that the even (respectively odd) sector converges to the Schrödinger theory with  $\theta = \pi/2$  ( $\theta = 0$ ). This convergence is consistent with what one would expect by inspection of the Schrödinger theory boundary condition (6.3).

### 6.3 Polymer half-line

We wish to modify the polymer Hamiltonian (6.10) to act on *one-sided* square-summable sequences, of the form  $c := (c_m)_{m=1}^\infty$  and with the inner product  $(d, c) = \sum_{m=1}^\infty \overline{d_m} c_m$ . We again choose the one-parameter family of modified Hamiltonians  $\{\hat{H}_\alpha \mid \alpha \in \mathbb{R}\}$  to be defined by adding at  $m = 0$  a fictitious lattice point with  $c_0 = \alpha c_1$ , so that

$$\begin{aligned} (\hat{H}c)_m = \frac{2}{\bar{\mu}^{3/2}} & \left[ \left( \left( m + \frac{1}{2} \right)^{1/2} + \left( m - \frac{1}{2} \right)^{1/2} + \frac{1}{4}\bar{\mu}^2 m^{1/2} \right) c_m \right. \\ & \left. - \left( m + \frac{1}{2} \right)^{1/2} c_{m+1} - \left( m - \frac{1}{2} \right)^{1/2} c_{m-1} \right] \quad \text{for } m > 1, \end{aligned} \quad (6.11a)$$

$$(\hat{H}c)_1 = \frac{2}{\bar{\mu}^{3/2}} \left[ \left( \left( \frac{3}{2} \right)^{1/2} + (1 - \alpha) \left( \frac{1}{2} \right)^{1/2} + \frac{1}{4}\bar{\mu}^2 \right) c_1 - \left( \frac{3}{2} \right)^{1/2} c_2 \right]. \quad (6.11b)$$

$E_0$

$\theta_P$ or $\theta$	0	$\pi/4$	$\pi/2$	$3\pi/5$	$4\pi/5$
$\bar{\mu} = 1$	1.23093	1.11371	0.904625	0.592200	–
$\bar{\mu} = 10^{-1}$	1.18178	1.04988	0.785426	0.423878	–
$\bar{\mu} = 10^{-2}$	1.16602	1.03780	0.770035	0.388607	–
$\bar{\mu} = 10^{-3}$	1.16113	1.03478	0.768373	0.380709	–
$\bar{\mu} = 10^{-4}$	1.15960	1.03390	0.768203	0.378624	–
Schrödinger	1.15890	1	0.768184	0.535489	–3.14921
$\theta_{\text{eff}}/\pi$	0	0.19527	1/2	0.636933	–

$E_1$

$\theta_P$ or $\theta$	0	$\pi/4$	$\pi/2$	$3\pi/5$	$4\pi/5$
$\bar{\mu} = 1$	1.87343	1.80220	1.72038	1.65342	1.39014
$\bar{\mu} = 10^{-1}$	1.84343	1.75446	1.63581	1.54923	1.32377
$\bar{\mu} = 10^{-2}$	1.83184	1.74589	1.62456	1.53274	1.30281
$\bar{\mu} = 10^{-3}$	1.82825	1.74396	1.62336	1.53023	1.29678
$\bar{\mu} = 10^{-4}$	1.82713	1.74343	1.62324	1.52975	1.29496
Schrödinger	1.82661	1.72401	1.62322	1.56006	1.34989
$\theta_{\text{eff}}/\pi$	0	0.19526	1/2	0.63692	0.84817

$E_2$

$\theta_P$ or $\theta$	0	$\pi/4$	$\pi/2$	$3\pi/5$	$4\pi/5$
$\bar{\mu} = 1$	2.34359	2.28992	2.23644	2.19574	2.00416
$\bar{\mu} = 10^{-1}$	2.32411	2.25111	2.16639	2.11021	1.95368
$\bar{\mu} = 10^{-2}$	2.31424	2.24373	2.15637	2.09634	1.93652
$\bar{\mu} = 10^{-3}$	2.31117	2.24216	2.15530	2.09435	1.93177
$\bar{\mu} = 10^{-4}$	2.31022	2.24174	2.15519	2.09401	1.93036
Schrödinger	2.30978	2.22684	2.15518	2.11361	1.97162
$\theta_{\text{eff}}/\pi$	0	0.19524	1/2	0.63691	0.84817

$E_3$

$\theta_P$ or $\theta$	0	$\pi/4$	$\pi/2$	$3\pi/5$	$4\pi/5$
$\bar{\mu} = 1$	2.73280	2.68919	2.64913	2.61958	2.46137
$\bar{\mu} = 10^{-1}$	2.72106	2.65720	2.58907	2.54603	2.42038
$\bar{\mu} = 10^{-2}$	2.71224	2.65049	2.57977	2.53351	2.40498
$\bar{\mu} = 10^{-3}$	2.70948	2.64911	2.57877	2.53177	2.40087
$\bar{\mu} = 10^{-4}$	2.70862	2.64875	2.57867	2.53148	2.39961
Schrödinger	2.70822	2.63625	2.57866	2.54653	2.43449
$\theta_{\text{eff}}/\pi$	0	0.19526	1/2	0.63691	0.84816

Table 2: The table shows the four lowest eigenenergies for the Einstein-Rosen wormhole throat, in the polymer theory as a function of the parameter  $\theta_P$  and the scale  $\bar{\mu}$ , and in the Schrödinger theory as a function of the parameter  $\theta$ . For each  $\theta_P$ , the polymer eigenenergies converge to those of the Schrödinger theory with  $\theta = \theta_{\text{eff}}$  as shown.

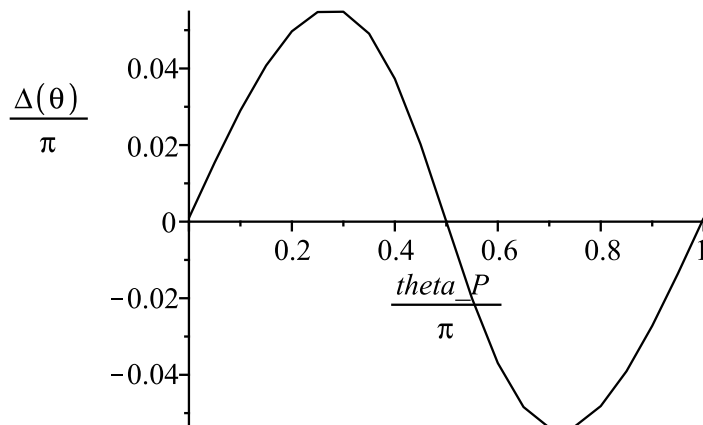


Figure 4:  $\Delta(\theta) := (\theta_P - \theta_{\text{eff}})$  is shown as a function of  $\theta_P$  for the Einstein-Rosen wormhole throat.

Each  $\hat{H}_\alpha$  is symmetric, and the coefficient of  $\overline{d_1} c_1$  in the inner product cannot be changed without losing this symmetry. The growth of the potential term suggests, by comparison with the solutions to the continuum eigenvalue equation, that each  $\hat{H}_\alpha$  is essentially self-adjoint; we have however not attempted to examine this rigorously.

We wish to examine the bound states in the limit  $\bar{\mu} \rightarrow 0$ . As in the previous cases, the key is to make  $\alpha$  depend on  $\bar{\mu}$  in a suitable way. Motivated by the continuum boundary condition (6.4), we introduce a parameter  $\theta_P \in [0, \pi)$ , and we choose

$$\alpha = \frac{\sin \theta_P}{\sqrt{\bar{\mu}} \cos \theta_P + \sin \theta_P}, \quad (6.12)$$

which is well defined for sufficiently small  $\bar{\mu}$  with any fixed value of  $\theta_P$ . Numerical results for the four lowest eigenvalues in terms of  $\theta_P$  are shown in Table 2.

For  $\theta_P = 0$  and  $\theta_P = \pi/2$ , the polymer eigenenergies converge to those of the Schrödinger theory with respectively  $\theta = 0$  and  $\theta = \pi/2$ : this reproduces the results found in the even and odd sectors of the real line polymer theory in [11]. For other values of  $\theta_P$  the polymer eigenenergies converge to those of the Schrödinger theory with  $\theta = \theta_{\text{eff}}$ , which differs from  $\theta_P$  as shown in Figure 4. Note that when  $\theta_P$  runs over the full interval  $[0, \pi)$ , so does  $\theta_{\text{eff}}$ .

If the limit  $\bar{\mu} \rightarrow 0$  is taken with  $\alpha = 1$ , it is seen from (6.12) and Table 2 that the polymer theory converges to the continuum theory with  $\theta = \pi/2$ , and if the limit is taken with any other fixed value of  $\alpha$ , the polymer theory converges to the continuum theory with  $\theta = 0$ . The continuum Dirichlet-type boundary condition hence again emerges as generic.

## 7 Conclusions

We have constructed a one-parameter family of polymer quantization Hamiltonians on the half-line. This family is mathematically analogous to the one-parameter family of Robin boundary conditions in Schrödinger quantization on the half-line. For the free particle, the attractive Coulomb potential and the Einstein-Rosen wormhole throat, we found that the full family of continuum Robin boundary conditions can be recovered in the continuum limit provided the polymer parameter is suitably fine-tuned, while without such a fine-tuning the continuum limit yields a Dirichlet-type continuum boundary condition. For the scale invariant potential the spectrum depends on the polymer scale only by an overall scaling, and a proper notion of a continuum limit does hence not exist, but even in this case the spectral properties revealed a close correspondence between the polymer theory parameter and the continuum theory boundary condition.

A notable feature of our half-line Hamiltonian is that it is well defined even when the classical potential function is singular at the origin, without any need to regularize the singularity. Mathematically, this feature arises because even though a fictitious lattice point at the origin was invoked to motivate the definition of the Hamiltonian, the actual value of the wave function at the origin never enters the theory, neither through the kinetic term nor through the potential term in the Hamiltonian. Physically, this feature is relevant to the issue of singularity resolution in polymer quantum gravity [25, 26] and may also have some impact in situations where polymer quantization is adopted as a regulator of ultraviolet divergences in quantum field theory [27].

One qualitative difference between the one-parameter family of continuum half-line Hamiltonians and our one-parameter family  $\{\hat{H}_\alpha\}$  of polymer half-line Hamiltonians is that the continuum parameter takes values in  $U(1) \simeq S^1 \simeq \mathbb{R} \cup \{\infty\}$  but our polymer parameter  $\alpha$  takes values in  $\mathbb{R}$ . While the definition (2.12) of  $\hat{H}_\alpha$  does as such not have a well-defined limit as  $\alpha \rightarrow \pm\infty$ , one could ask whether the (generalized) eigenstates of  $\hat{H}_\alpha$  might have an  $\alpha \rightarrow \pm\infty$  limit that is sufficiently regular for the family  $\{\hat{H}_\alpha\}$  to be completed into an  $S^1$ . Heuristically, thinking of  $\hat{H}_\alpha$  in terms of the fictitious lattice point at  $m = 0$  such that  $c_0 = \alpha c_1$ , the  $\alpha \rightarrow \pm\infty$  limit should mean taking  $c_1 = 0$ , which in turn should be equivalent to  $\hat{H}_0$  on a lattice that is shifted to the right by one step. For the free particle, we can verify from the analytic solution of Section 3 that this heuristics is correct: as  $\alpha \rightarrow \pm\infty$ , (3.9) shows that the bound state disappears, while (3.8) shows that states in the continuous spectrum have the limit  $\delta \rightarrow -\theta$ , which gives exactly the expected shift in  $m$  in (3.7). It would be interesting to examine whether the heuristics holds also for nonconstant potentials.

In all our examples, the parameter in the half-line polymer Hamiltonian affects the qualitative properties of the spectrum in a way that mimics closely the effects of the self-adjointness parameter in the continuum half-line theory. For example, for the free particle we saw that a single normalizable state can be made

to appear, and the energy of this state can be tuned to any value outside the continuous spectrum. This is just as in the continuum theory, the only difference being that the polymer continuous spectrum is an interval while the continuum continuous spectrum is half-infinite. As another example, we saw instances where adjusting the polymer parameter makes the lowest energy eigenvalue disappear while the higher eigenvalues each migrate downwards by one notch: similar behaviour occurs in the continuum theory. We were able to give a fully analytic description of these phenomena only for the free particle, but our numerical results suggest that it would be interesting to pursue an analytic description also for nonconstant potentials.

The results of our case studies are mutually compatible, and compatible with the continuum Schrödinger theory, to an extent that may exemplify a generic behaviour of the half-line polymer theory as a function of the parameter in the Hamiltonian. To examine this further, it would of course be of interest to extend the case case studies to wider classes of classical potentials, controlling both the analytic and numeric aspects. For example, one might want to consider the harmonic oscillator, for which the Schrödinger problem is readily analytically solvable in terms of parabolic cylinder functions [21]. We expect the half-line harmonic oscillator polymer theory to be related to the Schrödinger theory in a way qualitatively similar to what we found for the wormhole throat; however, we have not been able to develop a sufficient numerical control of the polymer theory eigenvalues to examine this question quantitatively.

## Acknowledgements

We thank Hanno Sahlmann, John Spevacek and an anonymous referee for useful comments, and in particular Don Marolf for raising the issue of the  $\alpha \rightarrow \pm\infty$  limit. This work was supported in part by the Natural Sciences and Engineering Research Council of Canada, by STFC (UK) and by the National Science Foundation under Grant No. NSF PHY11-25915. G. K. is grateful to the University of Nottingham for its hospitality during the initiation and completion of this work. J. L. thanks the organizers of the “Bits, Branes, Black Holes” programme for hospitality at the Kavli Institute for Theoretical Physics, University of California at Santa Barbara.

## References

- [1] M. Reed and B. Simon, *Methods of Modern Mathematical Physics II: Fourier Analysis, Self-adjointness* (Academic, New York, 1975).
- [2] J. Blank, P. Exner and M. Havlíček, *Hilbert Space Operators in Quantum Physics*, 2nd edition (Springer, New York, 2008).

- [3] G. Bonneau, J. Faraut and G. Valent, “Self-adjoint extensions of operators and the teaching of quantum mechanics”, *Am. J. Phys.* **69**, 322 (2001) [arXiv:quant-ph/0103153]; V. S. Araujo, F. A. B. Coutinho and J. F. Perez, “Operator domains and self-adjoint operators”, *Am. J. Phys.* **72**, 203 (2004); T. Fülöp, “Singular potentials in quantum mechanics and ambiguity in the self-adjoint Hamiltonian”, *SIGMA* **3**, 107 (2007) [arXiv:0708.0866 [quant-ph]].
- [4] B. Belchev and M. A. Walton, “Robin boundary conditions and the Morse potential in quantum mechanics”, *J. Phys. A* **43**, 085301 (2010) [arXiv:1002.2139 [quant-ph]].
- [5] A. Ashtekar, S. Fairhurst and J. Willis, “Quantum gravity, shadow states, and quantum mechanics”, *Class. Quant. Grav.* **20**, 1031 (2003) [arXiv:gr-qc/0207106].
- [6] H. Halvorson, “Complementarity of representations in quantum mechanics”, *Studies Hist. Philos. Mod. Phys.* **35**, 45 (2004) [arXiv:quant-ph/0110102].
- [7] T. Thiemann, *Modern Canonical Quantum General Relativity* (Cambridge University Press, Cambridge, 2007).
- [8] C. Rovelli, *Quantum Gravity* (Cambridge University Press, Cambridge, 2007).
- [9] V. Husain, J. Louko and O. Winkler, “Quantum gravity and the Coulomb potential”, *Phys. Rev. D* **76**, 084002 (2007) [arXiv:0707.0273 [gr-qc]].
- [10] G. Kunstatter, J. Louko and J. Ziprick, “Polymer quantization, singularity resolution and the  $1/r^2$  potential”, *Phys. Rev. A* **79**, 032104 (2009) [arXiv:0809.5098 [gr-qc]].
- [11] G. Kunstatter, J. Louko and A. Peltola, “Polymer quantization of the Einstein-Rosen wormhole throat,” *Phys. Rev. D* **81**, 024034 (2010) [arXiv:0910.3625 [gr-qc]].
- [12] G. Kunstatter, J. Louko and A. Peltola, “Quantum dynamics of the Einstein-Rosen wormhole throat,” *Phys. Rev. D* **83**, 044022 (2011) [arXiv:1010.3767 [gr-qc]].
- [13] T. Thiemann, “Quantum spin dynamics (QSD),” *Class. Quant. Grav.* **15**, 839 (1998) [arXiv:gr-qc/9606089].
- [14] G. Chacon-Acosta, E. Manrique, L. Dagdug and H. A. Morales-Tecotl, “Statistical thermodynamics of polymer quantum systems,” *SIGMA* **7**, 110 (2011) [arXiv:1109.0803 [gr-qc]].

- [15] E. Marinari and G. Parisi, “On polymers with long-range repulsive forces,” *Europhys. Lett.* **15**, 721 (1991).
- [16] J.-M. Lévy-Leblond, “Electron capture by polar molecules,” *Phys. Rev.* **153**, 1 (1967); O. H. Crawford, “Bound states of a charged particle in a dipole field,” *Proc. Phys. Soc. (London)* **91**, 279 (1967); C. Desfrancois, H. Abdoul-Carime, N. Khelifa and J. P. Schermann, “From  $\frac{1}{r}$  to  $\frac{1}{r^2}$  potentials: Electron exchange between Rydberg atoms and polar molecules,” *Phys. Rev. Lett.* **73**, 2436 (1994).
- [17] J. Gegenberg, G. Kunstatter and R. D. Small, “Quantum structure of space near a black hole horizon,” *Class. Quant. Grav.* **23**, 6087 (2006) [gr-qc/0606002]; G. Kunstatter and J. Louko, “Transgressing the horizons: Time operator in two-dimensional dilaton gravity,” *Phys. Rev. D* **75**, 024036 (2007) [gr-qc/0608080].
- [18] E. C. Titchmarsh, *Eigenfunction Expansions*, Vol. I, 2nd edition (Clarendon, Oxford, 1962).
- [19] S. Odake and R. Sasaki, “Discrete quantum mechanics,” *J. Phys. A* **44**, 353001 (2011).
- [20] C. J. Fewster, “On the energy levels of the hydrogen atom,” arXiv:hep-th/9305102.
- [21] *Digital Library of Mathematical Functions* (National Institute of Standards and Technology, Gaithersburg, Maryland, USA, 2010), <http://dlmf.nist.gov/~>.
- [22] J. L. Friedman, I. H. Redmount, and S. N. Winters-Hilt (unpublished, 1993).
- [23] I. H. Redmount, talk given at the 3rd Midwest Relativity Meeting, Oakland, Michigan, 1993.
- [24] J. Louko and J. Mäkelä, “Area spectrum of the Schwarzschild black hole”, *Phys. Rev. D* **54**, 4982 (1996) [arXiv:gr-qc/9605058].
- [25] M. Bojowald, “Loop quantum cosmology,” *Living Rev. Rel.* **8**, 11 (2005) [gr-qc/0601085].
- [26] A. Ashtekar and P. Singh, “Loop quantum cosmology: a status report,” *Class. Quant. Grav.* **28**, 213001 (2011) [arXiv:1108.0893 [gr-qc]].
- [27] G. M. Hossain, V. Husain and S. S. Seahra, “Background independent quantization and wave propagation,” *Phys. Rev. D* **80**, 044018 (2009) [arXiv:0906.4046 [hep-th]].